(Received 30 March 2026, Accepted 20 May 2026, Scheduled 3 June 2026)

A Fractal-Inspired Owl-Eye Circular Patch Antenna with Polygonal Defected Ground Structure for 3.6 GHz/4.6 GHz 5G and WLAN Applications

Lanka Padmalatha[1, 2, *], Satya N. Bhavanam[3], and Vasuja D. Midsala[3]

[1]*ECE Department, Acharya Nagarjuna University, Acharya Nagar, Guntur, Andhra Pradesh, India*
[2]*ECE Department, Seshadri Rao Gudlavalleru Engineering College, Gudlavalleru, Andhra Pradesh, India*
[3]*Department of CSE, Mangalyatan University Jabalpur (MUJ), Madhya Pradesh, India*

ABSTRACT: An owl-eye circular patch antenna with a polygonal defected ground structure (DGS) is presented in this paper for dual-band applications. The polygonal defected ground structure improves impedance matching and radiation characteristics, leading to a better gain and more efficient signal radiation. The design is fabricated on an FR-4 substrate measuring $35 \times 33 \times 1.6\,\text{mm}^3$. This is a cheap way to make modern wireless devices. Adding circular fractal features resembling an owl-eye pattern to the radiating element improves the current flow and enables multiple resonant modes. It works at 3.68 GHz and 4.68 GHz, which makes it suitable for 5G and WLAN applications. Antenna impedance matching is good, with reflection coefficient values of -24 dB at 3.68 GHz and -16 dB at 4.68 GHz. As a result, very little signal is reflected. At the frequencies where it operates, it achieves gains of 6.2 dBi and 5.68 dBi. Additionally, the antenna has a high radiation efficiency of about 95%, which means that it radiates well. Next-generation wireless communication systems will benefit from the proposed design.

1. INTRODUCTION

This paper describes an X-shaped fractal antenna along with a defective ground structure (DGS) for multiband application with broad bandwidth. The fractal design gives redundant current paths, allowing the possibility of more than one resonant frequency, and the DGS provides a wider bandwidth with better impedance matching. These features contribute to an improved radiation performance and reduced return loss, thus making it suitable for contemporary wireless communication applications [1]. To enhance the design, a fractal-based DGS is subsequently optimized using particle swarm optimization (PSO). This method allows for reducing the antenna size by approximately 69% with no penalty in impedance matching and radiation efficiency. Besides, the fractal DGS contributes further gain and bandwidth, indicating its suitability for microstrip patches in wireless applications [2]. In this paper, a novel gain flexible Koch fractal antenna embedding with a defective ground structure (DGS) for wearable Ka-band 5G applications is proposed. The multiband operation and compact size are empowered by fractal geometry, whereas the improved impedance matching and radiation efficiency are achieved due to DGS. The antenna is realised on a flexible substrate, making it appropriate for wearable and body-oriented communication systems [3]. Furthermore, a hybrid fractal antenna with a DGS is proposed and optimized using iterated function systems (IFSs) and artificial neural networks (ANNs). This method allows for multiband operation over the S, C, and X frequency bands and gain and bandwidth improvements. AI-based optimization techniques can be further applied to highlight the capabilities of intelligent methods, which proved that these fractal and DGS-based concepts may help work well even together [4]. In this paper, a Koch fractal antenna with controllable flexibility and a DGS is proposed for 5G Ka-band wearable applications. Fractal geometry assists compact size and multiband operation, while DGS enhances impedance matching and radiation efficiency. The antenna is able to be designed on a flexible substrate, making it ideal for wearable and body-centric communication systems [5]. Moreover, a hybrid fractal antenna with a DGS is designed and optimized by using both IFSs and ANNs. This allows multiband performance over S, C, and X frequency bands, along with gain and bandwidth improvements. It emphasizes the concept of fractal and DGS with AI-based optimization techniques, which are intelligent tools to improve antenna performance [6]. For Mobile Satellite Applications, the study presents compact square and hexagonal antennas with a Koch fractal-based defected ground structure (DGS). Such an approach allows for antenna miniaturization, along with desired circular polarization and gain; the DGS is very effective in enhancing bandwidth and impedance performance. Ultra-wideband fractal antennas with elliptical defected ground structures (DGSs) have also been reported for 5G millimetre-wave systems. In summary, these works show that the incorporation of various fractal geometries with DGS techniques may help reduce antenna size while improving bandwidth and radiation characteristics, whereas the latest research concentrates more on flexibility, AI tuning for complex mod-

* Corresponding author: Lanka Padmalatha (padmalatha4810@gmail.com).

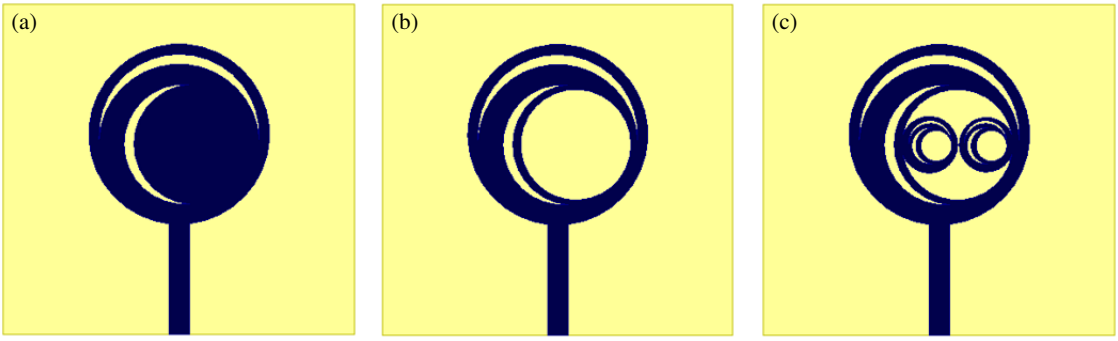

FIGURE 1. Design of fractal-inspired owl-eye-shaped antenna. (a) Iteration 1, (b) Iteration 2, (c) Iteration 3.

elling, 5G/6G higher-frequency applications [7, 8], etc. For wideband and space applications, antennas, such as circularly polarized inverted-F antennas [9] and hybrid fractal slot antennas [10], have been developed, providing stable performance over a wide frequency range. Additional studies include compact circular fractal antennas and Fibonacci-based fractal designs, which help reduce antenna size while maintaining broadband characteristics [11, 12]. Furthermore, modified Sierpinski and other fractal ground structures have been used to achieve multiband and quad-band operation for future wireless systems [13]. Fractal antennas have also been reported for applications such as RFID, WiMAX, and WLAN, with improved radiation efficiency and gain performance [14, 15]. In recent years, multi-fractal geometries combining two or more fractal concepts have been proposed to achieve high gain and wide bandwidth for modern communication systems [16]. Overall, these studies demonstrate that the integration of fractal geometries with defected ground structures is an effective approach to reduce antenna size and improve bandwidth, gain, and radiation performance. However, there is still a need for compact antenna designs that provide stable dual-band operation with simple geometry and efficient power performance for practical 5G and WLAN applications. While there are a vast number of fractal and DGS antennas reported, the previous designs are mostly designed on well-established geometries, namely Koch, Sierpinski, or rectangle-shaped slots. Such methods are generally multiband in nature but do not allow controlled tuning of resonant frequencies and may cause a larger antenna profile, complex design. Unexpectedly, bio-inspired circular fractal geometries combined with non-conventional defected ground structures for integration into compact dual-band applications have not been studied extensively. In order to overcome these shortcomings, this paper presents an owl-eye-inspired radiator based on the approach of fractality and combined this third-order DGS with a polygonal DGS for compact size, better reflective/broadcasting characteristics above the measured band, and stable radiation performance. A new kind of radial symmetric fractal radiator inspired from the owl eye is reported, and it greatly improves surface current distribution and allows controlled dual-band operation. The polygon DGS (defected ground structure) is proposed to improve the impedance matching as well as radiation properties. The miniaturized antenna, which has the dimension of $35 \times 33 \times 1.6\,\text{mm}^3$ can be used for sub-6 GHz wireless device applications. A dual-band antenna operating at 3.68 GHz and 4.68 GHz exhibits high radiation efficiency (∼95%) and stable gain performance. The proposed design is experimentally verified using measured results, which match well with the simulation.

2. FRACTAL-INSPIRED ANTENNA DESIGN DESCRIPTION

The proposed antenna is designed on an FR-4 substrate with overall dimensions of $35 \times 33 \times 1.6\,\text{mm}^3$. The iteration development is shown in Fig. 1. A circular radiating patch is modified by introducing smaller circular elements that form an owl-eye-inspired fractal shape (Fig. 2), which helps create additional current paths on the radiator. These circular features increase the effective electrical length and allow the antenna to produce two resonant frequencies. The structure is excited using a microstrip feed line that provides proper impedance matching for efficient power transfer. In addition, a polygonal defected ground structure is etched on the ground plane to improve impedance behavior and radiation performance of the antenna.

The functioning principle of the proposed antenna is featured in the fractal radiator along with a defected ground structure. A basic resonant mode is supported in the first circular patch. There is an increase in the electrical length of the current path with circular fractal elements and consequently, a new resonant mode is excited. The change in ground current distribution, as well as the presence of additional inductive and capacitive effects that are incorporated by the polygonal defected ground structure (DGS) leads to better impedance matching and thus, enhances bandwidth. The mutual coupling action between the fractal geometry and DGS facilitates dual-band stability at 3.68 GHz and 4.68 GHz, respectively. The proposed antenna dimensions are listed in Table 1.

The operation of the proposed antenna is determined by the fractal radiator and defected ground structure. The idea starts from a basic circular patch, which supports one mode. The circular fractal elements increase the effective electrical length, which gives rise to one more resonant frequency.

In addition, the polygonal DGS changes the ground plane current distribution, which supports impedance matching and bandwidth augmentation. However, the contribution of both

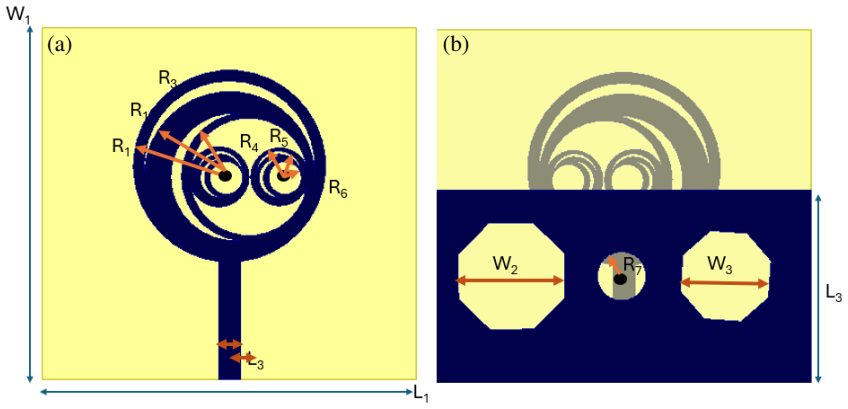

FIGURE 2. Design with all parameters in 2D view. (a) Front and (b) back view.

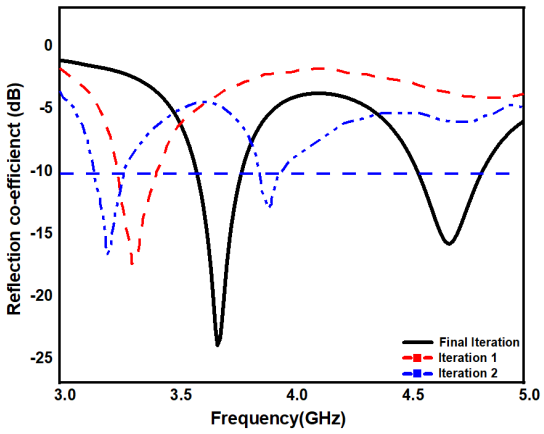

FIGURE 3. Proposed antenna iteration process.

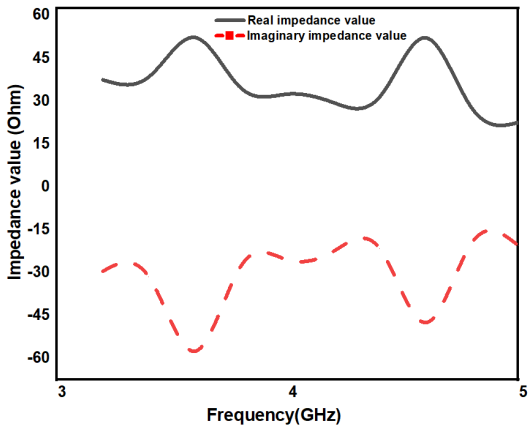

FIGURE 4. Impedance matching of the proposed antenna.

TABLE 1. Optimized dimensions of fractal-inspired antenna (mm).

Dimension	Value (mm)	Dimension	Value (mm)
L_1	33	R_2	15
W_1	35	R_3	11
L_2	2	R_4	2.8
L_3	18	R_5	2.1
W_2	9.9	R_6	1.8
R_1	17.5	R_7	2.2

the fractal geometry and the DGS in interplay allows dual-band stable performance at 3.68 GHz and 4.68 GHz.

3. RESULTS AND DISCUSSION

The graphic displays the antenna's reflection loss (S_{11}) performance throughout several design iterations. The antenna shows shallow resonances and does not consistently fulfil the -10 dB impedance matching criteria over the intended band in Iterations 1 (red line) and 2 (blue line). The Final Iteration (black) produces deeper resonant notches around 3.6 GHz and 4.6 GHz, suggesting better impedance matching. Reduced reflection and efficient power radiation are confirmed by reflection coefficient values that are much below -10 dB. It shows that the antenna's operating performance within the specified frequency range is much improved by the iterative design approach in Fig. 3.

When the antenna's impedance is equal to, or very near, the transmission lines or source's impedance — typically 50 Ω in radio frequency (RF) systems — this is known as impedance matching. Power is delivered from the source to the antenna with the least amount of signal reflection when impedance is matched. The proposed antenna's computed and measured impedance matching properties for the 3–5 GHz frequency range are displayed in the figure. Simulation and experimental validation are in high agreement since the measured result (black line) closely resembles the calculated one (red dashed line). Effective impedance matching (Fig. 4) with the conventional transmission line is confirmed by the impedance values approaching 50 Ω at 3.68 GHz and 4.68 GHz. The major causes of the small differences in the curves are measurement environment effects, connection losses, and fabrication tolerances. Overall, the findings confirm the suggested antenna design's dependability and viability.

The antenna is modelled using the equivalent circuit model (Fig. 5) that relates the antenna as a parallel combination of multiple RLC branches, with every branch representing one resonant mode of the antenna. We have inductance due to the current going on the conductive paths and capacitance from the patch and ground gaps and also inside the slot regions. The re-

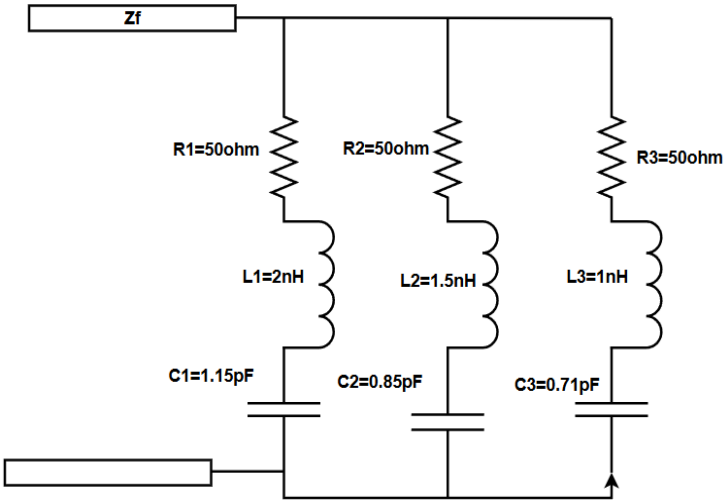

FIGURE 5. Equivalent circuit of proposed antenna.

sistance includes radiation and dielectric losses. The first RLC branch works for the lower resonant frequency (3.68 GHz), which is largely determined by the overall patch structure, and the second can be modelled as a higher resonant frequency (4.68 GHz), influenced by the fractal elements.

The circuit shown in Fig. 5 depicts a feeding impedance Z_f coupled to a parallel multi-branch RLC resonant network. It is divided into three branches, each of which contains inductors (L1, L2, L3), capacitors (C1, C2, C3), and resistors (R1, R2, R3) connected in series between the top and bottom wires. RLC branches function as resonant circuits, with resistors regulating bandwidth and damping, and inductors and capacitors storing electric and magnetic energy, respectively. Because the branches are connected in parallel, each branch can resonate at a distinct frequency based on the selected values of R, L, and C. Such networks are widely utilized in RF and antenna systems to achieve impedance matching, signal filtering, and support multiple frequency bands.

Figures 6(a)–(d) present a parametric study of antenna reflection coefficient (S_{11}) in the 3–5 GHz frequency band with respect to modifying different structural parameters. Fig. 6(a) shows that changing the width of the substrate (35–37 mm) has a significant effect on the depth of resonances, with 35 mm giving rise to the deepest. Fig. 7 shows the influence of substrate length (33–35 mm). As shown in Fig. 6(b), the reflection coefficient at a substrate length of 33 mm reaches values below -10 dB across working bands. The ground plane length has been modified in Fig. 2 (18–20 mm). Fig. 6(c) gives better impedance matching with its unique resonant dips. Comparing the 17.5 mm and 19.5 mm circular slot diameters in (d) demonstrates that wider diameter slots provide better impedance matching to strong resonance characteristics at lower frequencies due to a larger distance between conductors [3]. Overall, the results, in terms of resonant frequencies and impedance matching performance, show that the substrate dimensions, ground plane length, and slot diameter are the major contributors.

Figure 7 shows the reflection coefficient value of the proposed antenna at its operating frequency, i.e., representing the reflection coefficient values of -28.5 dB and -18.2 dB at frequencies 3.68 GHz and 4.68 GHz, respectively. The antenna is studied for 5G applications over n78 and n79 bands.

Simulated and measured gains across the 3–5 GHz frequency range are shown in the figure to confirm the dual-band operation of the proposed antenna. The measured gains are still a little less than the simulated values, as shown in Fig. 4: gain peaks at approximately 3.68 GHz and 4.68 GHz with measurements of around 6.0 dB and 5.5 dB, respectively; computed values reach roughly 6.3 dB and 5.8 dB of normalized gain at the same frequencies. The gain levels fall off between these frequencies, indicating high band selectivity and low radiation away from resonant regions. The reliability of the design is evidenced by the close match between measured and simulated results, with minor differences attributed to measurement losses and manufacturing tolerances. Overall, the antenna demonstrates a stable and efficient gain response, which makes it capable for use in valuable wireless applications, such as WLAN and 5G, as illustrated in Fig. 8.

The 3D radiation gain patterns of the proposed antenna at 3.68 GHz and 4.68 GHz are illustrated in Fig. 9(a). At 3.68 GHz, the antenna radiates an omnidirectional pattern with a maximum gain of 6.2 dB and a minimum value of -12.5 dB, showing the effective radiation in most directions [12]. The same radiation property can be detected from Fig. 9(b). In Fig. 9(b), the same radiation property can be detected at the higher operating band (4.68 GHz), with a peak gain of approximately 5.68 dB and -7.5 dB as the minimum value, which indicates the stability of its radiation characteristics in the higher operating band. This pattern validates that the antenna has stable radiation characteristics, and the gain pattern remains well distributed at both working frequencies, which qualifies this antenna for sub-6 GHz-based wireless communication applications.

Figure 10 presents the calculated and measured 2D radiation patterns of the proposed antenna at 3.68 GHz and 4.68 GHz at both $\Phi = 0°$ and $\Phi = 90°$ planes. Results of the quasi-

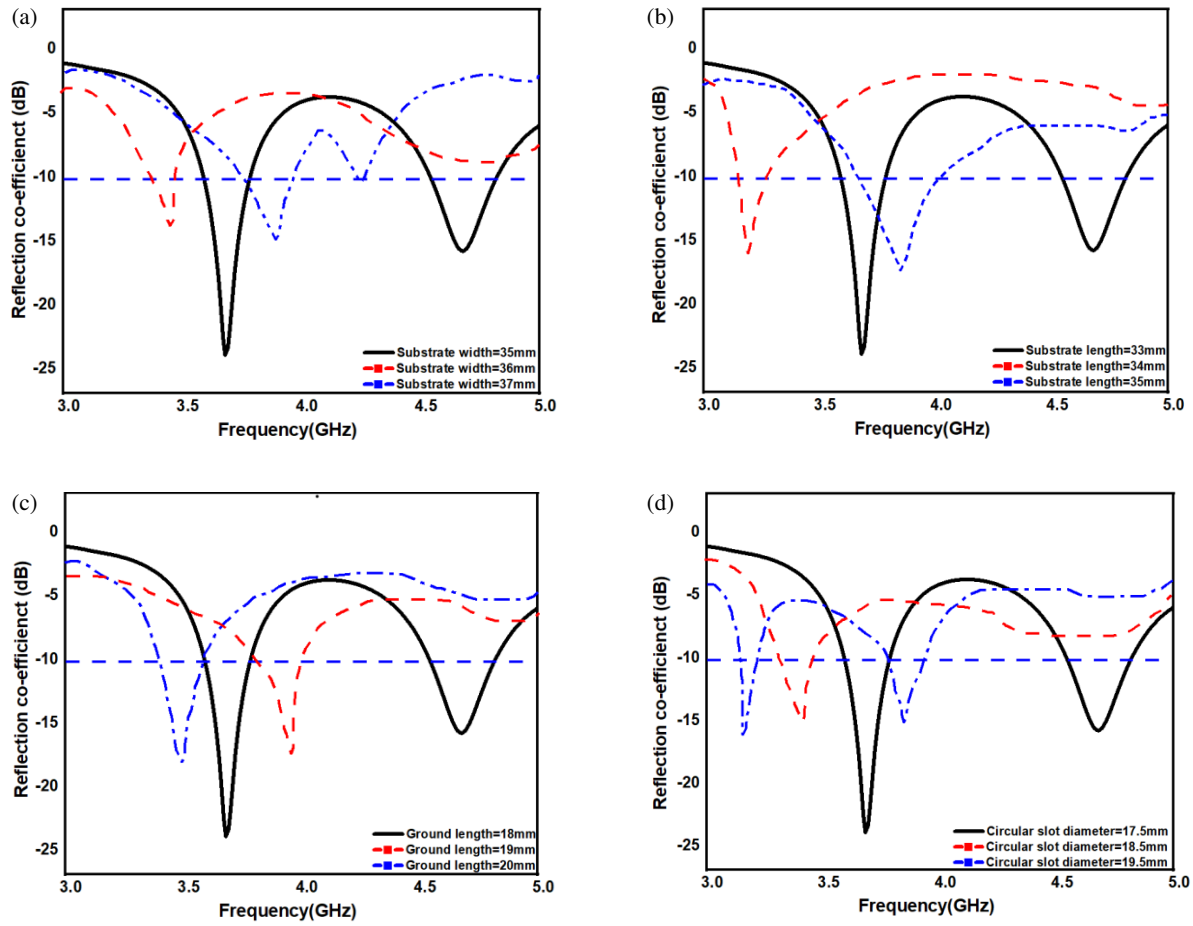

FIGURE 6. Parametric analysis of proposed antenna.

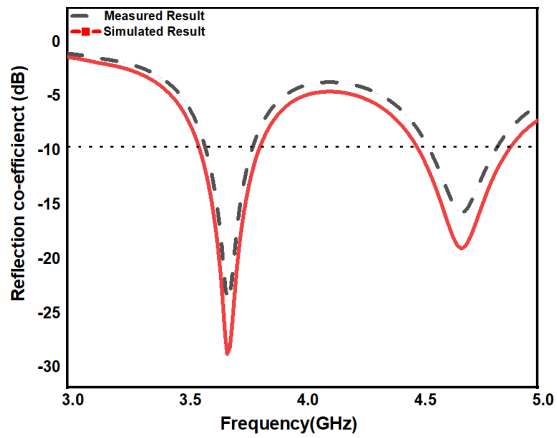

FIGURE 7. Reflection coefficient value of the proposed antenna.

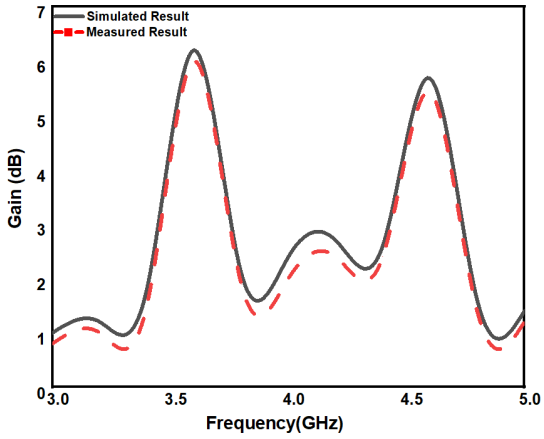

FIGURE 8. 2D gain value of the proposed antenna.

omnidirectional feature at 3.68 GHz are illustrated in Fig. 10(a), and the simulated result is close to the measured ones, which suggests that excellent agreement between simulation and measurement could be obtained. As shown in Fig. 10(b), the antenna exhibits a near-isotropic radiation property at 4.68 GHz. The closeness between the simulated and measured radiation patterns corroborates the reliability of the antenna performance and its stable pattern characteristics at both operational frequencies.

Figure 11 shows the electric field (E field) distribution of the introduced antenna at (a) 3.68 GHz and (b) 4.68 GHz. The electric field distribution plots at both frequencies show that most of the discrete energy is concentrated near the feed line and around the periphery of the circular radiating patch, which indicates the proper excitation of the antenna structure. There is also higher field intensity at the slot edges, which produces the resonant behaviours of these filter types. For example, it shows the proper radiative characteristics with a gradual decay

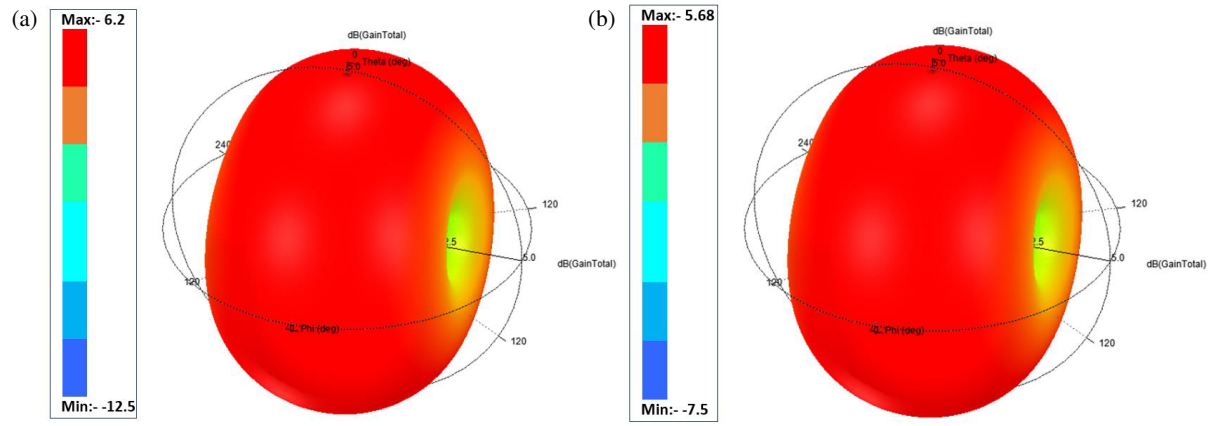

FIGURE 9. 3D gain value of the proposed antenna across the operating frequency.

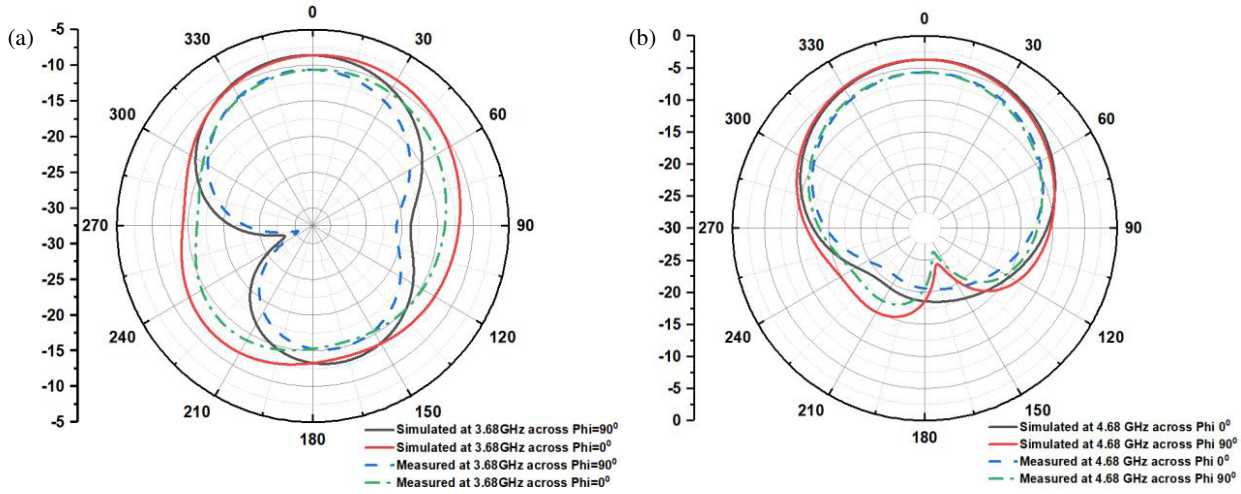

FIGURE 10. Radiation pattern value of the proposed antenna across the resonating frequency.

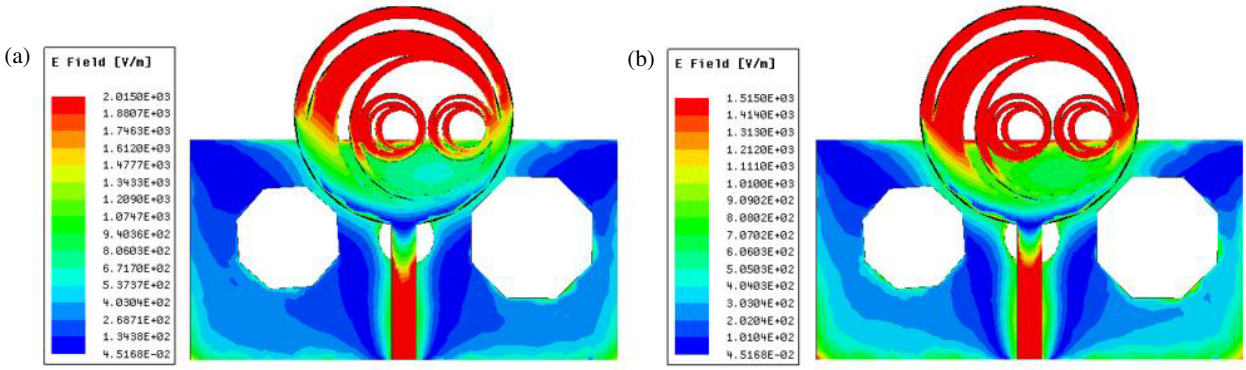

FIGURE 11. E-field distribution of the proposed antenna across the resonating frequency.

of field magnitude across the substrate toward its outer edges. This field pattern validates that the antenna structure allows for dual-band operation at the intended frequencies.

Figure 12 shows the computed magnetic-field (H-field) distribution of the designed antennas at (a) 3.68 GHz and (b) 4.68 GHz, respectively. It is clearly observed that surface currents properly flow around the circular radiating patch, feed line, and also in the slot area at both frequencies, as represented by a very dense magnetic-field concentration. The dense magnetic-field concentration around the patch edges and slot regions thus sets the resonant characteristics of the antenna. Higher field intensity near the patch edges and slots is an important parameter in determining this. The magnetic field intensity is slowly weakened over the substrate as it gets further

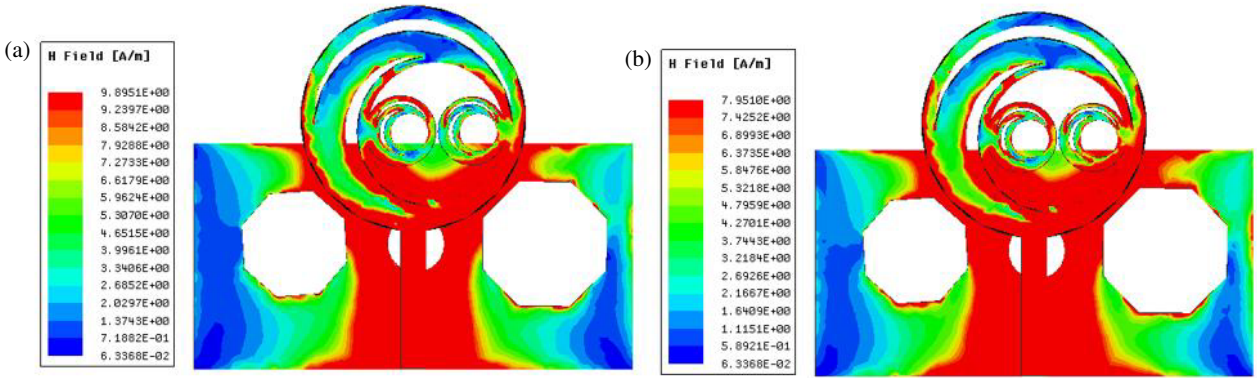

FIGURE 12. H-field distribution of the proposed antenna across the resonating frequency.

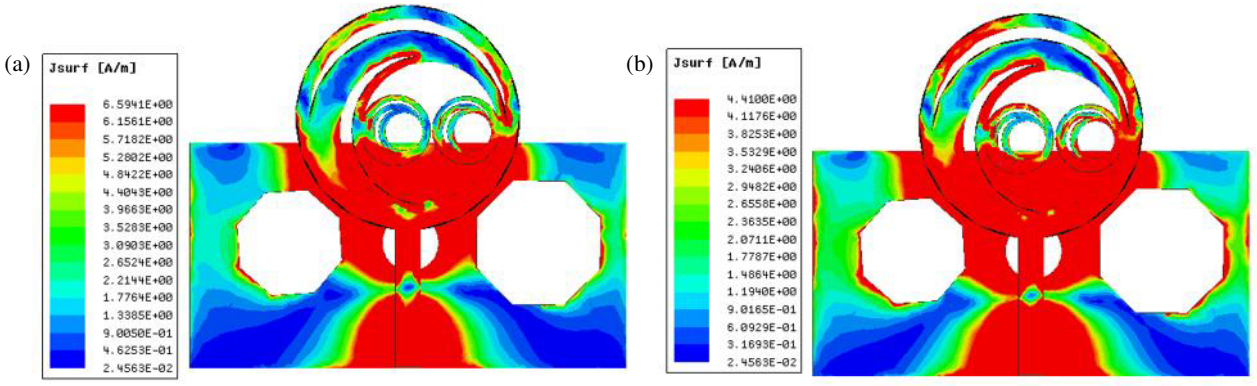

FIGURE 13. Surface current distribution of the proposed antenna across the resonating frequency.

away from the radiating structure. This is in line with the in-situ loading of the RF circuit layer on the antenna structure during operation, showing that it gives rise to stable radiation and efficient dual-band emissions at the marked resonant notch frequencies.

Figure 13 shows the surface current distribution on the proposed antenna (a) at 3.68 GHz, (b) at 4.68 GHz. The regions with efficient surface current flow include around the circular radiating patch, feed line, and slot areas at both frequencies, leading to the strong concentration of the surface current around these zones. The high field intensity close to the patch edges and slots is contributive to defining the resonant properties of the antenna. The surface current strength decreases continuously in the substrate with increasing distance from the radiating structure. This indicates that the antenna geometry does help to radiate with stability and support dual-band operation at those two resonance frequencies. Fig. 14 shows the radiation efficiency of the suggested antenna. The radiation efficiency value of the proposed value has been reported by the antenna mainly at the range of 95–98%. The value of 95% is attributable to the proposed antenna across the operating frequency 3.68 GHz, while the value of 98% is attributed to the proposed antenna across the operating frequency 4.68 GHz. The fractal-inspired antenna compared with other works is illustrated in Table 2.

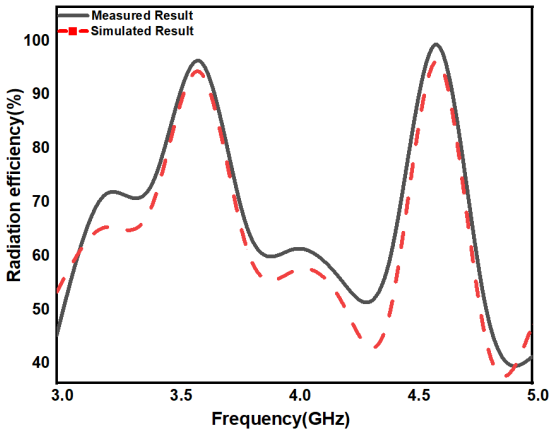

FIGURE 14. Radiation efficiency of the proposed antenna.

Better surface current concentration is presented along the outer edges of the circular patch and feed line at 3.68 GHz, thus suggesting that the lower resonance is primarily dictated by the overall radiator geometry. It gives the confirmation that the newer resonance is controlled by the self-similar arrangement of fractal elements at 4.68 GHz as the current distribution mostly concentrates around the inner circular fractal elements, as well as slot region. Such behavior is indicative that the geometry described promotes effective control of a multiresonant system.

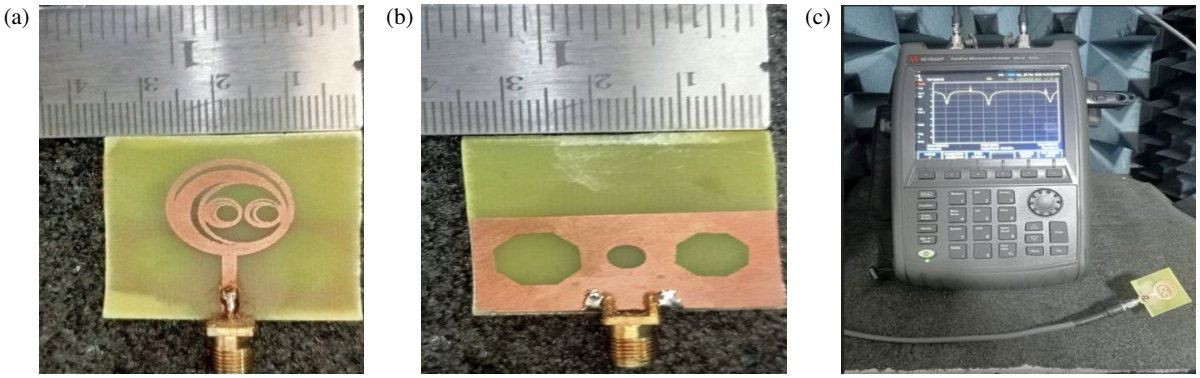

FIGURE 15. (a) Front view and (b) bottom view of the proposed design and (c) measuring analysis of the proposed antenna.

TABLE 2. Comparison of fractal-inspired antenna with previous works.

Ref.	Antenna Size (mm^2)	Frequency (GHz)	Gain (dBi)	Application
[9]	60×60	5.1 to 7 GHz	3	Multiband
[10]	38×38	3.6 4.9 5.9	3 3.2 4.2	WiMax, ISM
[11]	48×60	3.1–10.6	2.98	Wireless communication
[12]	100×100	2.7–14	1	Multiband
[13]	50×50	3.8–3.89 5.19–5.35 5.9–6.3 6.63–6.9	4.5	n78 Wifi C band
[14]	40×44	1.9–3.7 2.2–3.4	5	RFID WiMax WLAN
[15]	40×45	3.79 5.5	6	WiFi
[16]	40×50	2.45 3.43 7.69 8.25 9.79	NA	RADAR
This work	35×33	3.6 4.6	6.2 5.86	5G WLAN

3.1. Fabricated Model of the Proposed Antenna

Because it directly affects whether the antenna performs as intended in real-world scenarios, fabrication is crucial. Efficiency, dependability, and practical application are largely dependent on precision, material quality, and production processes.

Figure 15 shows the manufactured prototype of the antenna along with the measurement instrument: (a) The front view of the antenna with easily identify feed line and radiating patch, ground plane structure with defective geometries to enhance performance parameters, such as bandwidth and impedance matching from the back side of the antenna in (b). The conducting elements in the core of the antenna are made by printing copper on a dielectric substrate. (c) connectivity to a vector network analyzer (VNA) type instrument, which monitors metrics like reflection coefficient (S_{11}) of the constructed antenna output. This measurement setup ensures that the antenna's actual functioning matches its design expectations in a real-world scenario.

From a practical perspective, an FR-4 substrate is employed, which has low cost and is appropriate for mass-production applications. The small form factor and basic shape make it easy to integrate into new-generation wireless systems. These results indicate that the proposed antenna can be practically realized and is reliable for practical use.

Table 2 explains that the proposed antenna obtains a suitable compromise among miniaturization, gain, and efficiency. The antenna gives high gain in addition to small dimensions and high radiation efficiency, relative to previously used designs. This enhanced performance results from incorporating fractal geometry into a polygonal DGS.

Future work aims to implement reconfigurable components and investigate low-loss substrates in order to achieve improved performance for superior frequency applications.

4. CONCLUSION

The pseudo-fractal owl-eye radiator allows dual resonant frequencies to be created while the overall antenna structure remains concisely minimized. This benefits the gain and radiation behaviour of the antenna with better impedance match, i.e., a large contribution towards increasing launching efficiency in signal propagation is achieved by the proposed ground structure. It will enable one to generate the radiating element by integrating the circular fractal structure resembling an owl-eye-like features, which subsequently aid in achieving a better surface current distribution with multiple resonant modes. The simulated antenna is optimized for 3.68 GHz and 4.68 GHz operation, suitable for WLAN as well as 5G applications. The values of reflection coefficient are -24 dB at 3.68 GHz and -16 dB at 4.68 GHz, suggesting that the device is well matched in impedance and receives less signal reflection. It yields realized gains of 6.2 dBi and 5.68 dBi, respectively, at the operating frequencies.

REFERENCES

[1] Gupta, A., H. D. Joshi, and R. Khanna, "An X-shaped fractal antenna with DGS for multiband applications," *International Journal of Microwave and Wireless Technologies*, Vol. 9, No. 5, 1075–1083, 2017.

[2] Kakkar, S. and S. Rani, "A novel antenna design with DGS for emergency management," *International Journal of Applied Electromagnetics and Mechanics*, Vol. 42, No. 4, 629–637, 2013.

[3] Jilani, S. F., A. K. Aziz, Q. H. Abbasi, and A. Alomainy, "Ka-band flexible Koch fractal antenna with defected ground structure for 5G wearable and conformal applications," in *2018 IEEE 29th Annual International Symposium on Personal, Indoor and Mobile Radio Communications (PIMRC)*, 361–364, Bologna, Italy, 2018.

[4] Sran, S. S. and J. S. Sivia, "ANN and IFS based wearable hybrid fractal antenna with DGS for S, C and X band application," *AEU — International Journal of Electronics and Communications*, Vol. 127, 153425, 2020.

[5] Kalaiyarasan, R., G. Nagarajan, and S. Seenuvasamurthi, "Design and implementation of an efficient Sierpinski carpet fractal antenna with defected ground structure for 2.45 GHz applications," *e-Prime — Advances in Electrical Engineering, Electronics and Energy*, Vol. 6, 100320, 2023.

[6] Yuliandoko, H., E. Setijadi, and P. Handayani, "Dual band implantable antenna based on DGS and Sierpinski carpets fractal miniaturization," in *2024 IEEE Asia-Pacific Microwave Conference (APMC)*, 1126–1128, Bali, Indonesia, 2024.

[7] Praveena, H. D., K. Sudha, P. Geetha, and I. Suneetha, "A compact square and hexagonal antennas with fractal DGS for mobile satellite applications," *Journal of Pharmaceutical Negative Results*, Vol. 13, No. 4, 2022.

[8] Sharma, A., A. Baliyan, K. kharb, and M. G. Siddiqui, "Ultra-wideband fractal antenna with elliptical defected ground structure on Rogers RT/Duroid 6002 for 19.75–23.46 GHz and 27.25–36 GHz 5G mm-Wave bands," *International Journal of Advances in Signal and Image Sciences*, Vol. 12, 839–849, 2026.

[9] Behera, H. K., M. Midya, and L. P. Mishra, "Circularly polarized inverted F antenna for UWB application," *Materials Today: Proceedings*, 2023.

[10] Singh, S., A. Varshney, V. Sharma, I. Elfergani, C. Zebiri, and J. Rodriguez, "A compact off-set edge fed odd-symmetric hybrid fractal slotted antenna for UWB and space applications," *Progress In Electromagnetics Research B*, Vol. 102, 37–60, 2023.

[11] Dastranj, A., F. Ranjbar, and M. Bornapour, "A new compact circular shape fractal antenna for broadband wireless communication applications," *Progress In Electromagnetics Research C*, Vol. 93, 19–28, 2019.

[12] Tirado-Mendez, J. A., D. Martinez-Lara, H. Jardon-Aguilar, R. Flores-Leal, and E. A. Andrade-Gonzalez, "Inscribed Fibonacci circle fractal in a circular radiator for ultra-wideband antenna operation and size reduction," *International Journal of Antennas and Propagation*, Vol. 2019, No. 1, 6393401, 2019.

[13] Kale, P. D., S. B. Patil, P. V. Deshmukh, D. P. Tulaskar, V. Bhope, D. Parkhi, Y. Thakare, and A. K. Shahade, "A novel quadband antenna with circular patch and modified Sierpinski Gasket fractal ground structure for next-generation wireless communication system," *Journal on Wireless Communications and Networking*, Vol. 2026, 35, 2026.

[14] Wang, E., X. Liu, and H. Chang, "Wideband circular polarized fractal antenna for RFID/WiMAX/WLAN applications," *Progress In Electromagnetics Research Letters*, Vol. 111, 111–120, 2023.

[15] Desai, A., T. K. Upadhyaya, R. Patel, S. Bhatt, and P. Mankodi, "Wideband high gain fractal antenna for wireless applications," *Progress In Electromagnetics Research Letters*, Vol. 74, 125–130, 2018.

[16] Azzouz, A., R. Bouhmidi, M. E. Munir, M. M. Nasralla, and M. Chetioui, "Performance analysis of a high-gain multi-band wheel-shaped fractal antenna using Sierpinski carpet and Koch snowflake geometries," *Results in Engineering*, Vol. 26, 105328, 2025.